



INFORME TÉCNICO SOBRE EL NIVEL DE RUIDO EN LAS MEDIDAS AC EN LOS EQUIPOS MPMS-5S Y MPMS-XL

INFORME DIRIGIDO A LOS USUARIOS DE LOS
MAGNETÓMETROS SQUID

Contenido:

- [1. Introducción](#)
 - [2. Signal Nulling y Nulling Amplitude](#)
 - [3. Resultados experimentales con muestra](#)
 - [4. No sample Test](#)
 - [5. Deriva del SQUID](#)
 - [6. Conclusiones](#)
- Apendice
-

SIC-MF-2007.05.23-I06

A. Arauzo
Servicio de Instrumentación Científica – Área de Medidas Físicas. Universidad de
Zaragoza, Pedro Cerbuna 12, 50009 Zaragoza.

1. Introducción

La opción de medida de susceptibilidad AC en los magnetómetros MPMS dotados con un sensor SQUID, permite realizar medidas de alta precisión con una sensibilidad de hasta 1×10^{-8} emu en el rango 0.1 Hz hasta 1 kHz.

En los casos en los que la máxima sensibilidad se requiere, el sistema tiene que estar optimizado para bajar el nivel de ruido al mínimo permitido por el instrumento. Este nivel puede estar limitado por el efecto de acoplamiento de ruidos externos al sistema, así como por la precisión de los componentes electrónicos y la estabilidad geométrica de las bobinas de excitación y detección.

Para determinar el nivel de ruido en los sistemas existentes en el Servicio, MPMS-5S y MPMS-XL, se han realizado varias pruebas. Por una parte se han realizado medidas experimentales con una muestra que da una señal muy pequeña y que precisa de la máxima sensibilidad del sistema, y por otra se ha realizado un test básico de determinación del nivel de ruido del sistema. Asimismo se ha comprobado la velocidad de deriva del sensor SQUID de ambos equipos para comprobar que presenta valores comparables.

2. Signal Nulling y Nulling amplitud

La sensibilidad máxima posible con las medidas AC basadas en un detector SQUID sólo se pueden conseguir si se reducen señales de fondo parásitas y efectos espúreos. Para esto, el sistema AC del MPMS, alimenta el circuito superconductor de entrada con señales que automáticamente anulan el offset DC, ruido de la línea a 50 Hz, así como la señal del campo AC aplicado que se ve en el gradiómetro (señal AC de excitación). Para ello el sistema utiliza respectivamente el DC offset Nulling, Line Nulling y Drive Nulling.

El DC offset Nulling, cancela el offset DC. Si no fuera así, la resolución de digitalización quedaría reducida a 5 mV, unas 100 veces la sensibilidad del sistema. El sistema añade una señal proporcional al offset a las otras señales (line Nulling y Drive Nulling). Se realiza automáticamente durante el line nulling, drive nulling y al principio de cada medida AC.

Line Nulling anula el ruido de la línea de alimentación a 50 Hz, que típicamente es de 5×10^{-6} emu pico a pico para la frecuencia principal. Este ruido limitaría la resolución a 0.5 – 1 mV, que es un orden de magnitud mayor que el ruido del SQUID. Se realiza automáticamente durante el primer centrado o medida AC después de un encendido.

Drive Nulling cancela las señales debidas a la señal de excitación AC, desbalanzas del gradiómetro y momento de la muestra. Para ello, el sistema calcula de forma iterativa una forma de onda que anula la señal AC vista por el gradiómetro. El proceso se repite hasta que la amplitud de la señal es menor que el parámetro 'null amplitude'. Normalmente el sistema utiliza 3 a 4 iteraciones para obtener 5×10^{-8} null para un campo de excitación de 1 G. Se realiza antes del centrado o de una medida. Esta señal de anulado también cancela el offset DC y el ruido de la línea. Drive nulling asegura medidas muy precisas aunque alarga el proceso de medida. El proceso puede reducir la señal AC residual en el sistema de detección del SQUID cuatro órdenes de magnitud, dando lugar a un rechazo de la señal de excitación AC de 1 en 10^7 .

El Drive Nulling no es preciso realizarlo durante el centrado AC ya que incrementa innecesariamente el tiempo de centrado.

En una medida AC estándar, se realiza una medida en dos puntos y se aplica una señal de anulado en ambas. En la primera posición, centrada en la bobina inferior de la bobina captora, se calcula la señal de anulado como aquella que cancela la señal completamente, incluida la señal de la muestra. En la segunda posición, centrada en la bobina media de la bobina captora, se aplica una señal de anulado idéntica a la anterior, con lo que la señal de la muestra se ve incrementada un factor tres, dada la polaridad de las bobinas (+1 -2 +1). Esta medida es la que utiliza el sistema para determinar la susceptibilidad AC de la muestra.¹

Para medidas que requieran la máxima sensibilidad, la muestra se puede volver a centrar después de cada cambio en temperatura.

La 'Null Amplitude', es decir la amplitud máxima de la señal remanente que el sistema mide en el primer punto, es un parámetro que se define en cada medida AC. El valor óptimo depende de la amplitud de la señal AC de excitación (Drive Amplitude) así como de la señal de la muestra. Valores muy pequeños respecto a la señal de la muestra pueden alargar mucho el tiempo de medida e incluso dar error, caso de

¹ Para información más detallada ver Apéndice: Rev. Sci. Instrum. 65(8), August 1994.

que el sistema no sea capaz de conseguir el nivel requerido. El proceso iterativo se repite hasta que la amplitud de la señal remanente es menor que la null amplitud, el regresión fit es menor que 0.001 o el número de iteraciones excede de 20. Valores grandes reducen la sensibilidad del sistema.

El valor óptimo de la 'Null Amplitude' es un valor aproximadamente igual a la señal de la muestra.

3. Resultados Experimentales con muestra

Se han realizado medidas en ambos equipos 5S y XL con una misma muestra (D4NOL-B) en función de la frecuencia y el número de bloques. Esta muestra tiene una señal muy débil y se quiere determinar en que condiciones se puede minimizar el ruido. En todas estas medidas se ha usado un drive nulling de 1×10^{-5} .

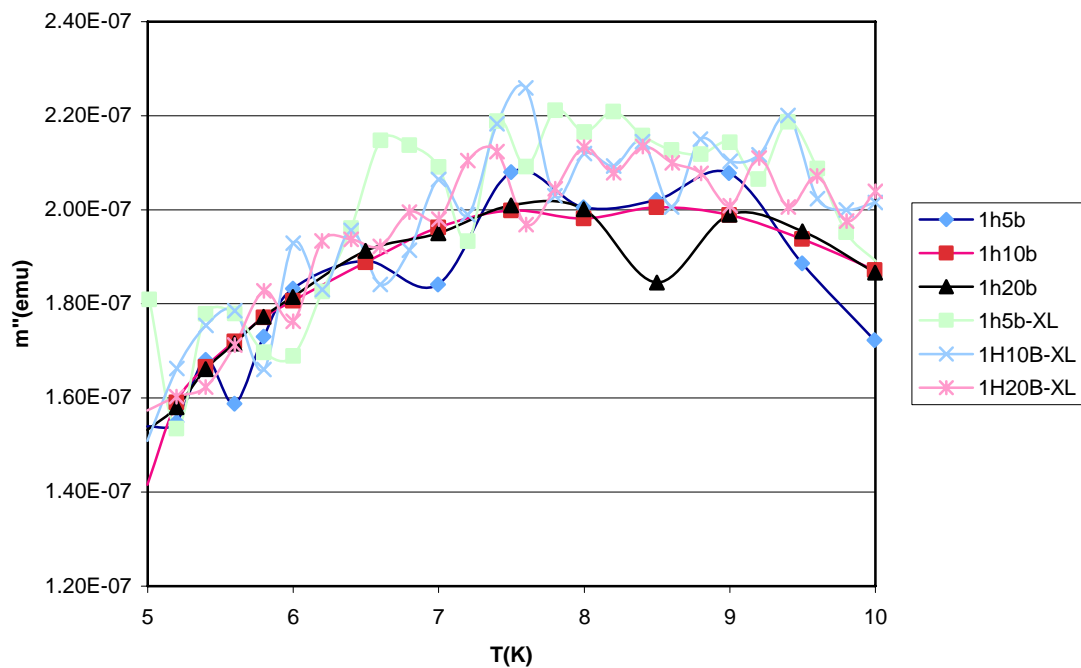


Figura1: Resultados de la medida en cuadratura del momento AC (m'') para 1 Hz para distinto número de bloques en los equipos MPMS-5S (' ') y MPMS-XL ('XL').

En estas medidas se observa que a 1 Hz, el resultado que presenta menos dispersión es el realizado en el equipo MPMS-5S para 10 bloques (ver Figura1). En cambio a 10 Hz, las medidas realizadas en el equipo MPMS-XL presentan en general menor ruido que las realizadas en el otro equipo.

A 120 Hz no se aprecian diferencias relevantes entre los resultados de ambos equipos.

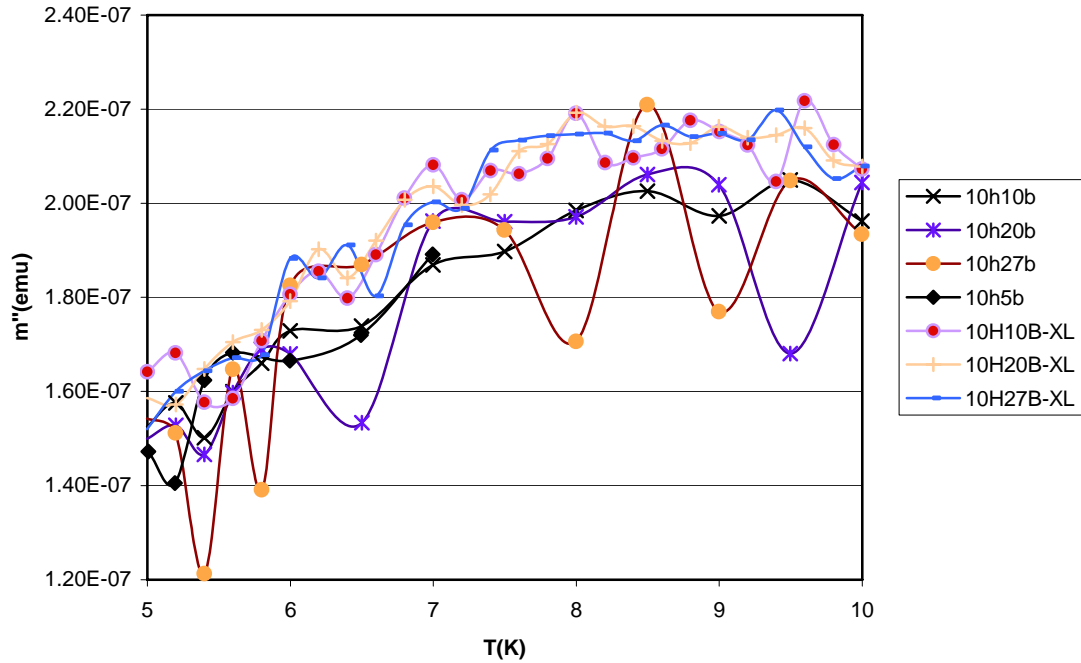


Figura2: Resultados de la medida en cuadratura del momento AC (m'') para 10 Hz para distinto número de bloques en los equipos MPMS-5S (' ') y MPMS-XL ('XL').

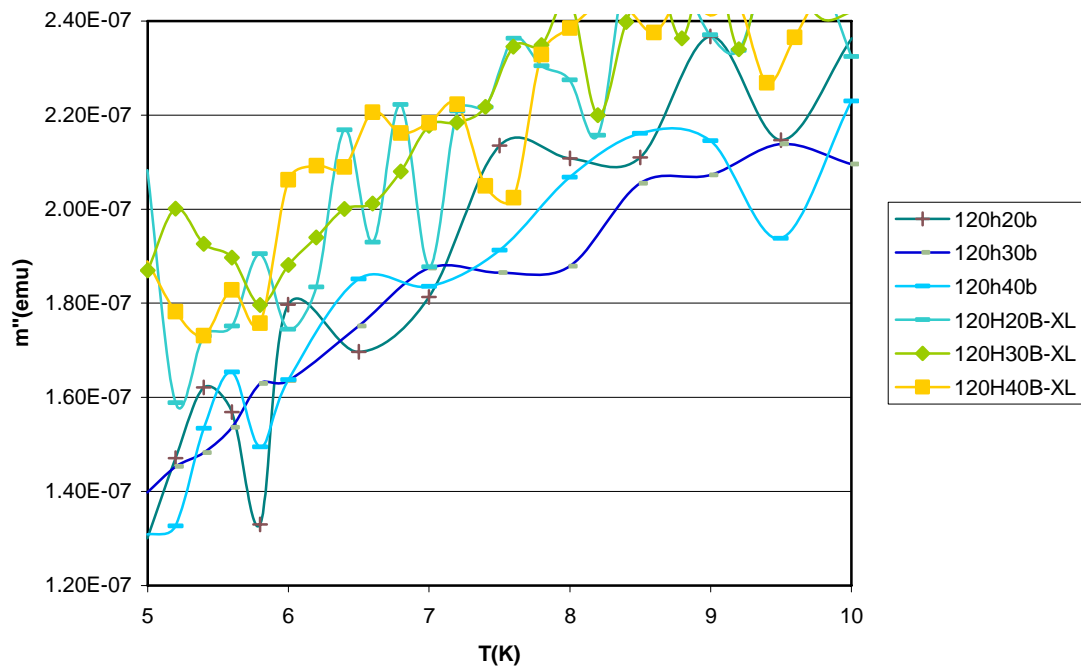


Figura3: Resultados de la medida en cuadratura del momento AC (m'') para 120 Hz para distinto número de bloques en los equipos MPMS-5S (' ') y MPMS-XL ('XL').

Como conclusión de estas medidas, no se puede decir que en general un equipo sea mejor que el otro. El 5S presenta los mejores resultados para medidas a 1 Hz, pero a 10 Hz parece mejor el XL. Estos resultados se pueden resumir en que, a priori, la medida a 1 Hz, 10 o 20 bloques (se ve peor la de 20, pero no hay resultados promedio) y en el equipo MPMS-5S es la que da menos nivel de ruido.

4. No sample Test

Este test permite observar si hay un nivel de ruido extra en un equipo debido a que el proceso de 'drive nulling', presenta algún problema. Para ello, se realizan medidas a distintas frecuencias, disminuyendo progresivamente la amplitud requerida para el nulling hasta el mínimo posible, 10^{-8} . Si el sistema es incapaz de llegar hasta este nivel da un error ('AC Drive Nulling Error').

También permite comparar las limitaciones de distintos instrumentos en función de la frecuencia y nivel de nulling.

Los resultados se muestran en las Figuras 4-7 para el equipo 5S y XL en función de la frecuencia y nivel de nulling. Solamente se ha observado que el sistema de un error en el caso del equipo 5S para 1 Hz y 10^{-8} nulling amplitud. En todas las medidas se ha usado una onda de excitación de 1 Oe de amplitud. Las medidas se han realizado a 6 K. El número de bloques promediado varía con la frecuencia, siendo de 1 bloque a 1 Hz, 5 bloques a 10 Hz, 10 bloques a 100 Hz y 20 bloques a 1000 Hz.

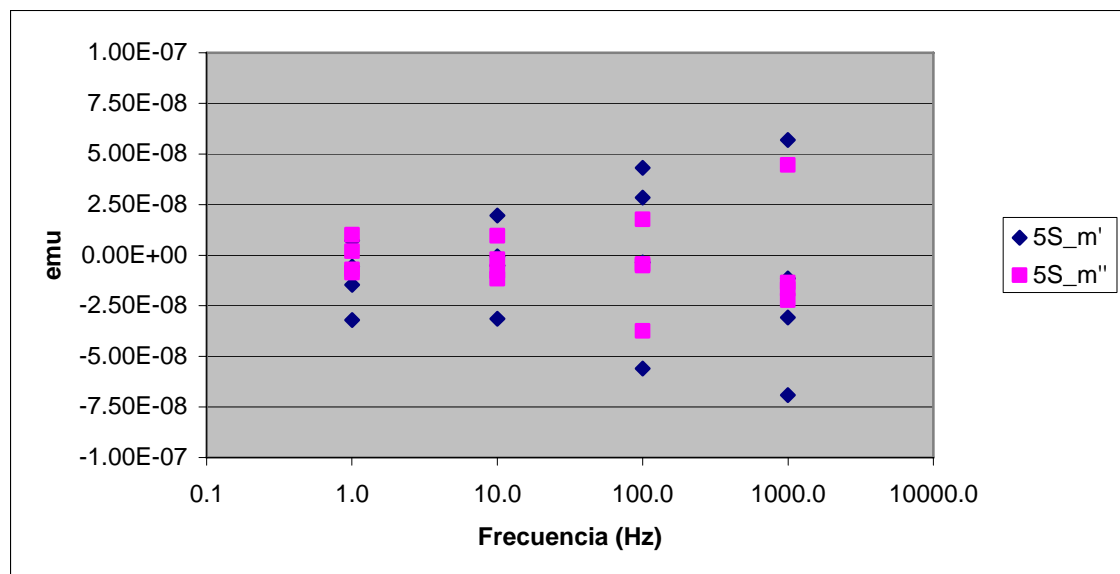


Figura4: Resultados de la medida AC sin muestra (Noise Background Level) en función de la frecuencia en el equipo MPMS-5S.

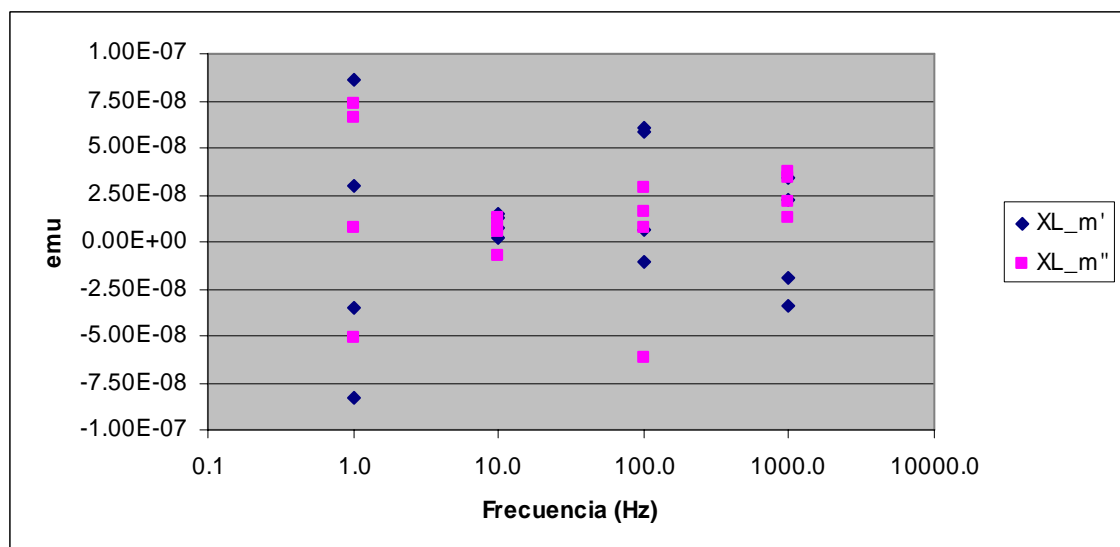


Figura5: Resultados de la medida AC sin muestra (Noise Background Level) en función de la frecuencia en el equipo MPMS-XL.

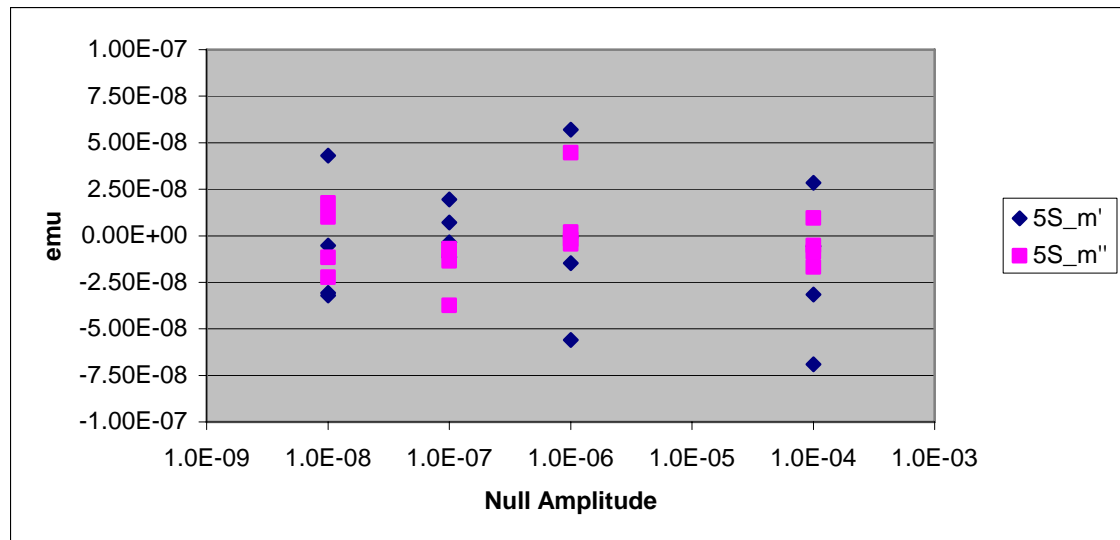


Figura6: Resultados de la medida AC sin muestra (Noise Background Level) en función de la Null Amplitude en el equipo MPMS-5S.

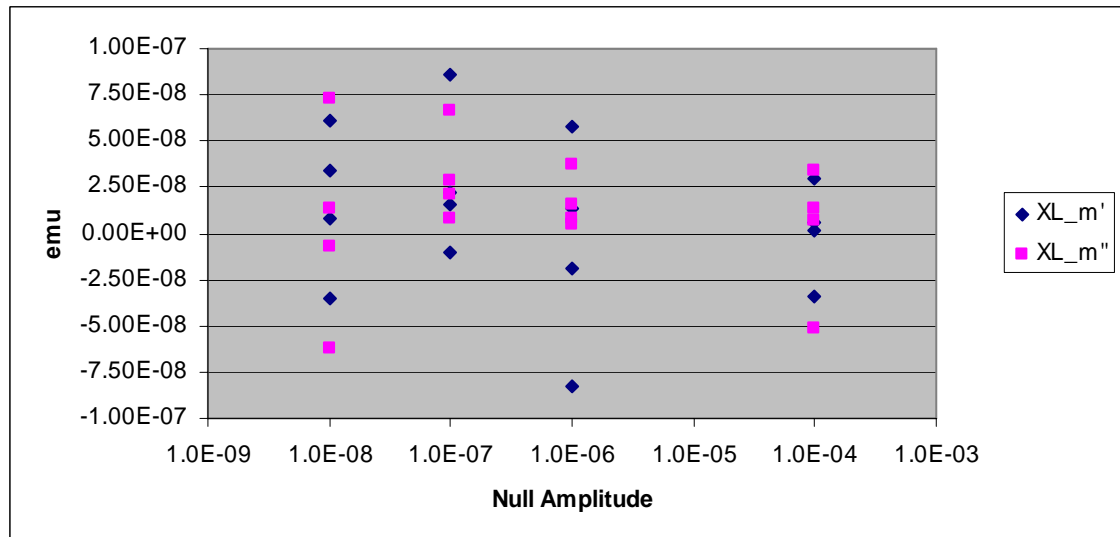


Figura7: Resultados de la medida AC sin muestra (Noise Background Level) en función de la Null Amplitude en el equipo MPMS-XL.

Los resultados en función de la 'null Amplitude' no son concluyentes. No parece que haya una correlación clara entre el nivel de ruido observado y el nivel de anulación del mismo. En cambio si que se observa una variación del ruido con la frecuencia. En el equipo 5S el nivel de ruido aumenta al aumentar la frecuencia entre 1Hz y 1000 Hz, en cambio en el equipo XL, los mejores resultados se obtienen para una frecuencia de 10 Hz.

5. Deriva del SQUID (Squid drift rate)

La deriva del Squid puede dar lugar a una fuente adicional de ruido. Una gran deriva es de esperar inmediatamente después de realizar una variación grande del campo magnético. Para minimizar este efecto conviene siempre poner el campo magnético en modo 'oscillate', el cual minimiza los efectos de relajación del campo magnético y por tanto la deriva producida en el sensor SQUID. Para disminuir aún más esta deriva, en el caso en que se vayan a hacer medidas que requieran la máxima sensibilidad del equipo conviene hacer lo siguiente:

Dejar el imán a campo cero durante una hora antes de comenzar la medida o realizar un Magnet Reset.

Se ha hecho un análisis de la velocidad de deriva del SQUID en condiciones de alta estabilidad del campo magnético con el objetivo de hacer una comparación de este efecto en ambos equipos, XL y 5S. Se ha obtenido un valor promedio de 15 mV/min en el equipo MPMS-XL y de aproximadamente 1 mV/min en el equipo MPMS-5S. Estos valores están dentro de lo esperado y no supone un aumento del nivel de ruido en ninguno de los dos equipos.

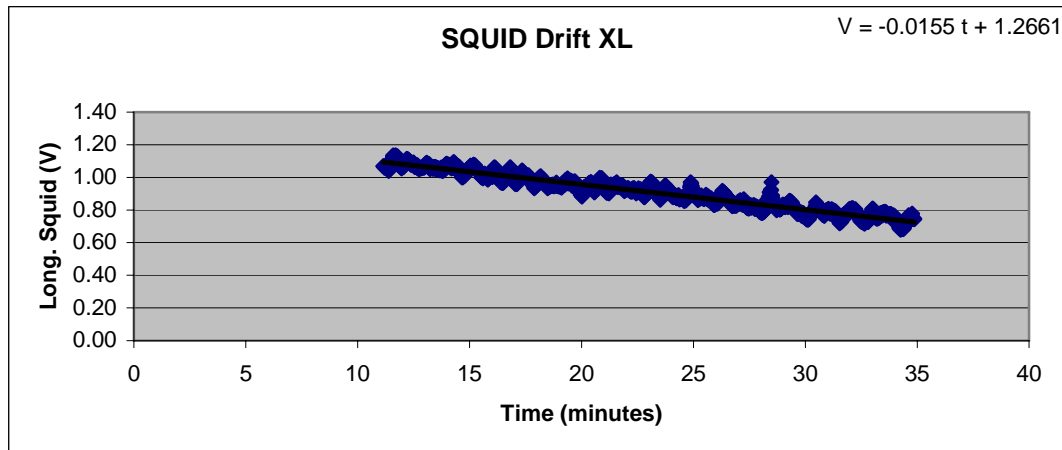


Figura8: Resultados de la medida AC sin muestra (Noise Background Level) en función de la Null Amplitude en el equipo MPMS-XL.

6. Conclusiones

De los tests realizados con y sin muestra se puede concluir que el nivel de ruido del sistema es del orden de $1 \cdot 10^{-7}$ o menor, y que es similar en ambos equipos MPMS-5S, y MPMS-XL.

Se ha encontrado una correlación del nivel de ruido con la frecuencia de excitación que permite a priori, escoger las condiciones de medida óptimas para cada equipo, que son 1 Hz para el MPMS-5S y 10 Hz para el MPMS-XL.

Las recomendaciones adicionales para medir muestras que requieren la máxima sensibilidad del sistema son las siguientes:

- Utilizar el valor óptimo de la 'Null Amplitude' (aproximadamente igual a la señal de la muestra).
- Volver a centrar después de cada cambio en temperatura.
- Dejar el imán a campo cero durante una hora antes de comenzar la medida o Realizar un Magnet Reset.
- En general, se consigue una mejora en la resolución en la amplitud de la señal medida incrementando el número de bloques a promediar conforme la frecuencia aumenta. Hay que tener en cuenta que cuando se opera a bajas frecuencias, si el tiempo de promediado es largo comparado con el tiempo de estabilidad del sistema (entre saltos de flujo del SQUID o debido a cambios térmicos), tiempos de promedio más largos pueden incrementar los errores de medida.

A SQUID-based ac susceptometer

A. D. Hibbs, R. E. Sager, S. Kumar, J. E. McArthur, and A. L. Singaas
Quantum Magnetics, Inc., 11578 Sorrento Valley Road, San Diego, California 92121

K. G. Jensen, M. A. Steindorf, T. A. Aukerman, and H. M. Schneider
Quantum Design, Inc., 11578 Sorrento Valley Road, San Diego, California 92121

(Received 13 September 1993; accepted for publication 4 May 1994)

We have developed a high-resolution ac susceptometer that uses a rf superconducting quantum interference device to directly measure the flux coupled into a superconducting detection coil from a sample's changing magnetic moment in an applied ac field. The system operates in a frequency range from 0.01 to 1500 Hz and an applied ac field range of 0.1–400 μT with a sensitivity of about $5 \times 10^{-12} \text{ A m}^2$ for magnetic moment measurement, and at a reduced sensitivity down to 0.001 Hz. The instrument is based on an existing dc magnetometer system and uses that system's temperature control and dc superconducting magnet to allow operation over a temperature range from 2 to 400 K and in applied dc fields of $\pm 5.0 \text{ T}$. During a measurement all operations are controlled automatically by computer from a menu-driven software system, with user input required only on initiation of a measurement sequence. Both real and imaginary components of the ac susceptibility can be determined.

I. INTRODUCTION

Both dc and ac methods of measurement are commonly used in determining magnetic properties of materials such as the magnetization M and magnetic susceptibility X . Magnetization is commonly determined through direct measurement of a sample's magnetic moment in a *dc magnetometer*. The most sensitive instruments available for dc magnetization measurements use a superconducting quantum interference device (SQUID).^{1,2} The SQUID acts as a flux-to-voltage convertor to directly measure the change in flux as the sample moves through a superconducting detection coil coupled to the SQUID. Commercial systems³ typically allow measurements to be performed over a wide range of temperatures and applied fields by providing for temperature control of the sample and including a superconducting magnet for applying a dc magnetic field. This allows dc magnetization curves to be generated and the static or dc susceptibility $X_{\text{dc}}=M/H$ to be determined.

While useful and often sufficient, the information from dc measurements is limited in that no information is obtained about the dynamics of the magnetic system. In an *ac susceptometer*^{4–12} an oscillating magnetic field is applied to the sample; the change in flux seen by the detection circuitry is due only to the changing magnetic moment of the sample as it responds to the applied ac field. The differential or ac susceptibility $X_{\text{ac}}=dM/dH$ obtained from these measurements is described as having both real and imaginary components X' and X'' , where the imaginary component is proportional to the energy losses in the sample. The complex susceptibility can provide information on properties such as structural details of materials, resonance phenomena, and electrical conductivity via induced currents; relaxation processes such as flux profiles and flux creep in superconductors, and energy exchange between magnetic spins and the lattice in paramagnetic materials.¹³

Conventional ac susceptometers measure the voltage induced in an inductive detection coil by an oscillating mag-

netic moment. Various designs for ac susceptometers have been reported in the literature. The most common systems use mutual inductance bridges^{4–7} to measure the voltages induced, and some use digital processing to improve noise rejection.^{6,14} Because these systems only measure signals with frequencies at or very near the applied excitation, the sensitivity is greatly increased over a dc magnetometer by reducing the effective noise level to that in the measurement bandwidth centered on the frequency of interest. However, these systems lose sensitivity at low frequencies because the voltage induced in the detection coil is proportional to the frequency of the oscillating drive field. A solution to this problem is to combine an ac drive field with a SQUID-based detection system. The frequency-independent coupling between magnetic flux and induced currents in superconductors allows one to use ac frequencies and ac drive fields many orders of magnitude lower than in conventional ac systems.

Such SQUID-based systems have been used for many years to perform low-frequency ac susceptibility measurements in a variety of special measurement applications.^{4–15} In this paper we describe a fully automated, general purpose SQUID-based ac susceptometer developed as an extension to an existing commercial dc magnetometer.³ Our system is capable of ac measurements of a sample's magnetic moment with a resolution of $5 \times 10^{-12} \text{ A m}^2$ over a frequency range of 0.01–1500 Hz with loss of sensitivity occurring only at frequencies below 0.01 Hz. The system operates over the temperature range 2–400 K and in applied dc fields up to $\pm 5.0 \text{ T}$. All operations during a measurement are controlled automatically by computer from a menu-driven software system, with user input required only on initiation of a measurement sequence. The combination of extremely high SQUID sensitivity and the noise rejection inherent in ac techniques offers the potential for performing extremely sensitive ac susceptibility measurements on systems such as spin glasses and other physical systems characterized by long relaxation times. The system is also ideal for samples where the material characteristics or magnetic effects under investigation

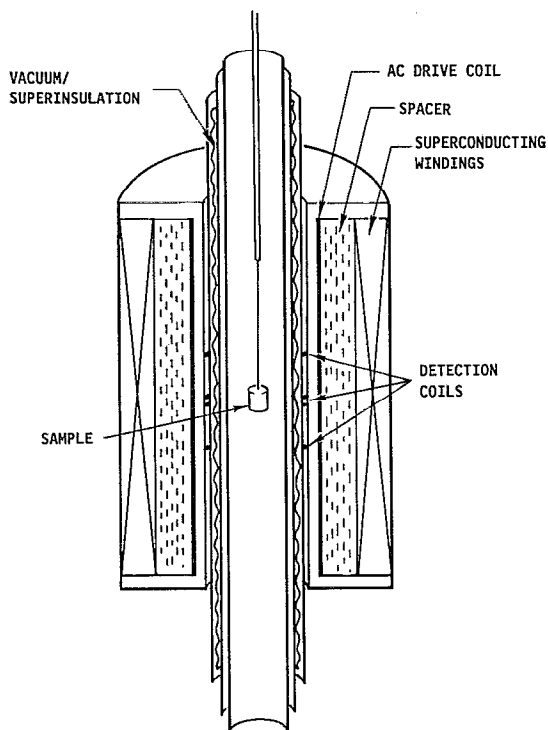


FIG. 1. Schematic of the lower portion of the SQUID ac susceptometer. The sample is thermally isolated from the detection coils, ac drive coil, and the superconducting windings.

require that very small excitation fields be used, as in measurements on high-temperature superconductors.

II. SYSTEM OVERVIEW

In this section we describe the overall design of the ac susceptometer system. Further details of the ac system's physical configuration that affect its calibration and its sensitivity under specific operating conditions are given in later sections.

A. Cryostat and sample insert

As shown in Fig. 1, the sample is suspended in a central chamber isolated from the liquid-helium bath, allowing the temperature of the sample to be controlled from 2 to 400 K while the ac drive coil, detection coils, and superconducting dc magnet remain at liquid-helium temperature. The ac drive field is supplied by a copper solenoid driven by a digital programmable waveform synthesizer. The amplitude of the ac field is adjustable over the range 0.1–400.0 μT and the frequency from 0.001 to 1500 Hz. The coil is concentric with the dc superconducting magnet, which is operated in persistent mode and can apply a maximum field of ± 5.0 T.

The superconducting detection coils, configured as a second-order gradiometer, are wound on the smallest possible diameter (2.8 cm) in order to obtain maximum coupling to the sample. To assure reproducibility of the measurements, the sample is centered in the detection coil before the measurements are made. This is accomplished by passing the sample completely through the gradiometer while measuring

the SQUID response. The measured data are fit to a theoretically predicted curve via a least-squares regression fit, with axial position as the variable parameter. The sample position thus derived allows one to calculate the displacement necessary to place it at the center of the appropriate coil of the gradiometer. The sample can be recentered after each temperature change for measurements requiring the highest sensitivity.

B. Operational overview

In order to take full advantage of the extreme sensitivity possible with SQUID-based ac measurements, it is necessary to reduce unwanted background signals and spurious effects. This function is performed automatically by the system and is transparent to the user. The primary reason for these operations is to allow the SQUID electronics to be set to their maximum sensitivity with respect to the sample magnetic moment. This is achieved by feeding signals back into the superconducting input circuit to actively cancel 60(50) Hz line noise, nulling any residual signal from the ac drive field caused by the (inevitable) imbalance in the gradiometer, and by cancelling the signal from the sample itself. Note that the sample is always exposed to the unmodified drive field, since the corrections are applied directly to the circuit connecting the gradiometer coils to the SQUID. The details of the electronics used to implement these sensitivity-maximizing procedures and the operation of the instrument during measurements are described in the next sections.

III. ELECTRONICS

A block diagram of the detection and SQUID control electronics is shown in Fig. 2(a). Magnetic flux from the sample is detected by a superconducting pickup coil, which is part of a closed-loop superconducting circuit inductively coupled to the SQUID. The feedback circuitry is also coupled to this circuit through a superconducting dc flux transformer. The voltage output from the SQUID electronics, which is proportional to the flux change in the detection coils, is digitized by the ac digitizer [Fig. 2(b)] and recorded in the computer. A current proportional to the signal voltage is created by the ac drive system [Fig. 2(c)] and can be fed back inductively into the superconducting input circuit through the feedback flux transformer, along with other noise-cancelling signals as described below.

The master timing signal for the system is a 12 MHz crystal oscillator, which is divided down to 6 MHz to drive the analog-to-digital (A/D) converter for the ac digitizer, and further to 3 MHz before being passed to the ac drive system.

A. ac drive

The ac drive system contains a ripple counter which divides down the incoming 3 MHz signal into five clock rates between 187.5 kHz and 2.861 Hz. These clock rates are used to drive two 16-bit waveform synthesizers, one for driving the solenoid which creates the ac magnetic field and the other for nulling the drive signal which couples to the SQUID via the gradiometer imbalance, as described in the next section. The synthesizers are based on a memory chip

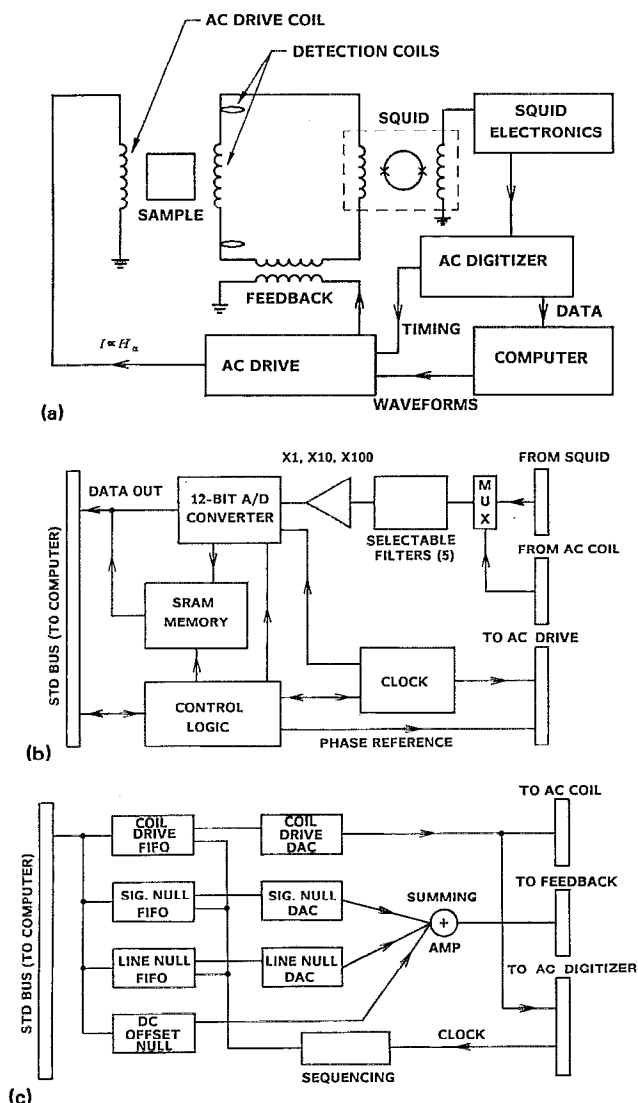


FIG. 2. (a) Overview of the measurement system and electronics, showing drive and pickup coils, SQUID detector and electronics, feedback coils, ac digitizer and drive systems, and computer used for control and data storage. (b) Block diagram of ac digitizer system showing the input from SQUID and ac drive coils, A/D converter, on-board memory, control logic, clock, and output to ac drive system. (c) Block diagram of ac drive system showing the FIFOs for storing digital waveforms from computer, DACs for producing the output to the ac drive coil and nulling signals, summing amp for feedback signals, and sequencing logic.

organized as a FIFO (first in, first out) buffer. The outputs of the FIFO are connected to a digital-to-analog converter (DAC) where the analog waveforms are generated and sent to the appropriate coils. Both channels contain differential amplifiers with ranges of $1\times$ and $100\times$ which are switched simultaneously, giving an effective resolution of 23 bits. The channels are clocked synchronously and contain the same number of points per output sine wave up to a maximum of 8192 points. To keep harmonics to an acceptable level, we use a minimum of 124 digital points for sine wave generation, depending on which of the five available clock rates are used. When phase shifts are required between the output of the drive and nulling channels they are produced by numerically offsetting the digital sine waves loaded into the FIFOs.

B. ac digitizer

The heart of the ac digitizer is a 12-bit A/D converter which digitally samples the voltage output of the SQUID electronics synchronous to the drive waveform synthesizer. Before being digitized, the signal is passed through an instrumentation amplifier with gains of $1\times$, $10\times$, and $100\times$, in addition to the range and gain settings of the SQUID electronics. Five selectable three-pole Butterworth filters provide antialiasing in addition to noise reduction. The filter rolloff frequencies were chosen to give small phase shifts ($<3^\circ$) at the maximum intended drive frequency for each sampling rate.

The data is stored in onboard memory and passed to the computer at the end of a measurement. The maximum number of wave periods digitized in a given measurement is determined by the size of the digitizer memory. A maximum of 65 535 16-bit data points can be stored on the board; this limits the maximum amount of averaging that can be used per measurement. Data recorded in blocks of two wave periods are transferred to the host computer, which adds the data from different blocks together point by point. This has the effect of averaging the background noise at a given data point. The amplitude and phase of the resulting two-cycle dataset are calculated using a regression algorithm with the known frequency as a fixed parameter. The calibrated phase and amplitude corrections are applied to the raw data and the in- and out-of-phase sample moments reported to the user via a choice of data files.

IV. SIGNAL NULLING

There are potential limitations when digitizing the sample signal due to the 12-bit resolution of the A/D converter used. Its resolution is only one part in 4096 which is considerably less than the dynamic range of the drive field. To make maximum use of the converter range, we actively cancel spurious instrument based and external signals as described below.

A. dc offset removal

To ensure that the full range of the converter is used, we must remove dc offsets from the data. The majority of the dc component of the sample's magnetic moment is removed when the SQUID electronics is reset. However, after the SQUID is reset there is always a residual dc voltage of order 0.1–5 V (on the most sensitive SQUID range and gain). If unmodified this offset clearly limits the digitizing resolution when the offset is larger than the sample signal. Thus a signal proportional to the dc offset is added to the other nulling signals in a summing amplifier and sent to the feedback flux transformer.

B. Line noise removal

The 60(50) Hz line noise is typically of order $100 \Phi_0$ and therefore limits the resolution of the digitized data. The line nulling circuitry uses a digital waveform synthesizer in the ac drive system [Fig. 2(a)] to create a signal 180° out of phase with the line voltage. The signal is phase locked to the line frequency and operates independently of the other chan-

nels. It is added to the imbalance nulling signal via the summing amplifier and sent to the feedback flux transformer with the other feedback signals. The line nulling is ordinarily performed only on first actuating the ac measurement protocol. It can be reselected by the user at any time, but experience has shown that remeasurement and recancellation is seldom necessary during a measurement sequence.

C. Gradiometer coupling to the applied field

The most significant problem in achieving the maximum sensitivity of an ac susceptometer is to cancel the direct coupling between the ac drive coil and the superconducting detection coils. The usual correction to this effect is to wind the coils as a gradiometer, which in the ideal case does not detect the spatially uniform ac magnetic field directly. We have chosen a second-order gradiometer configuration, which reduces somewhat the flux-coupling ability of the detection system but increases the rejection of spurious effects by also being insensitive to linear gradients in the field. However, small deviations in the projected areas of the gradiometer coils still limit the gradiometer balance to 0.1%–0.2%. For a 100 μT driving field, this corresponds to a flux coupled into the SQUID of about $2\Phi_0$, independent of the sample presence. This is the reason for the second waveform synthesizer in the ac drive system, identical to that driving the ac coil. Before each measurement the nulling circuitry injects a current (with an appropriate phase shift) directly into the feedback flux transformer that cancels both the signal due to the gradiometer imbalance and the signal resulting from the sample moment itself. The complete procedure for making a measurement is described in the next section.

When properly implemented, this technique can reduce the residual ac signal in the SQUID detection system by four orders of magnitude, providing a total rejection of the ac drive signal of order one part in 10^7 . It is important to note that the factor of 10 000 improvement obtained with the electronic feedback is possible to achieve using readily available precision electronic components. But for the system to maintain this rejection level for the drive field, the geometrical stability of the drive and detection coils must be stable to the level of rejection desired. The design shown in Fig. 1 makes this possible by making the ac drive coil an integral part of the superconducting dc magnet and then combining the magnet and detection coils into a completely monolithic structure. Since all of these elements reside in the liquid-helium bath, they remain at constant temperature throughout the measurements, minimizing phase shifts and changes in coil geometry as the sample temperature and magnetic field are varied.

V. OPERATION OF THE SUSCEPTOMETER

We now have all the elements necessary to describe the actual measurement procedure. The protocol is summarized in a flow chart in Fig. 3. The system executes this protocol automatically when a measurement sequence is initiated by the user. A high-order cancellation of the background response of the system is obtained using this technique.

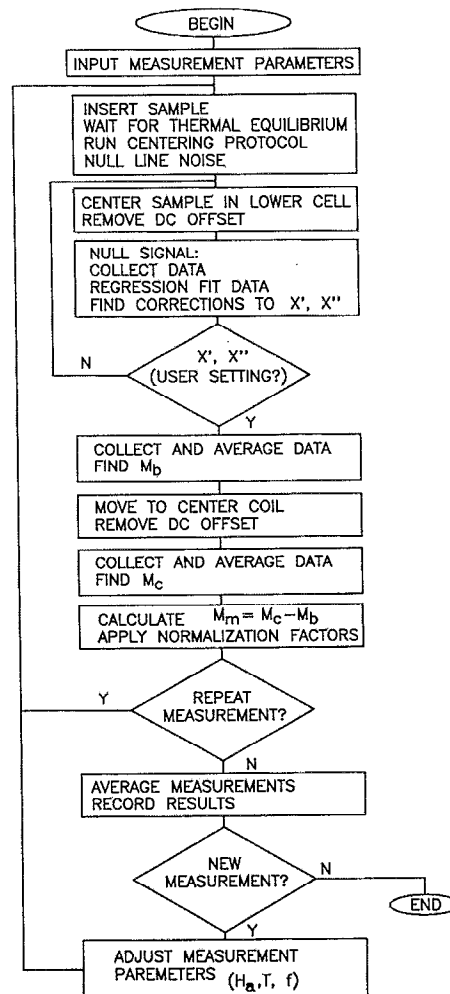


FIG. 3. Flow chart of experiment control protocol. See Sec. IV for details.

A. Measurement procedure

A standard measurement actually comprises two separate measurements, one in the lower gradiometer coil and one in the center coil. An alternative method for removing all instrumental effects would be to null the signal before the sample is inserted in the cryostat and make a single measurement in one detection coil. This method is inadequate for precision measurement due to variations in the temperature of the cryostat insert and vibration of the apparatus, which cause serious stability problems for the SQUID. Removing the sample from the detection coils would also require that the sample be removed from any applied dc magnetic field on each measurement.

Before the actual measurements are made, the sample is centered in the detection coils using the procedure described in Sec. I A above. The sample is then moved into the start position in the lower coil of the gradiometer. The system automatically nulls any line noise present if necessary (see Sec. III B) and removes the dc offset. The total signal resulting from gradiometer imbalance and the sample itself is now nulled to a preselected level by sending the appropriate nulling current to the feedback transformer as described in the previous section. Note that the signal need only be nulled to

a level approximately equal to that of the sample itself to allow the SQUID electronics to be set to their maximum sensitivity with respect to the sample moment. The remnant signal in the bottom coil M_b is then measured for a length of time specified by the user, averaged, and recorded in the computer. The data are then fit to the equation

$$M_b = A + Bt + M' \cos(\omega t) + M'' \sin(\omega t), \quad (1)$$

where A represents any remaining dc offset, B is a linear drift in the field or temperature, ω is the angular frequency of the ac driving field oscillation, and M' and M'' are proportional to that part of the in-phase and out-of-phase components that have not been completely removed from the measurement by the nulling procedure described above. The sample is then moved into the center coil of the gradiometer and the signal M_c measured. The data are again fit to Eq. (1). The difference between these two measurements is about three times the actual moment of the sample, since the center coil has the opposite orientation of the lower coil and twice as many windings. These two sets of data are of the form

$$M_b = Mf(b) + M_0, \quad M_c = Mf(c) + M_0, \quad (2)$$

where M is the actual moment of the sample, M_0 is any residual signal due to gradiometer imbalance, and $f(x)$ is a function of position along the central axis of the gradiometer. The function $f(x)$ is the (normalized) response function of the magnetometer to an idealized dipole at position x . If the sample is small compared to the dimensions of the pickup coil, it can be approximated as an idealized dipole. This function is determined analytically and verified in a separate measurement using the dc superconducting magnet. Each of the two components of the susceptibility are then calculated from the difference between the two measurements,

$$M = N \frac{M_c - M_b}{f(c) - f(b)}, \quad (3)$$

where N is an overall normalization factor for the amplitude of the moment. Because the sample moment is always measured at two positions in the sample space, the residual direct coupling M_0 is the same at both positions and is therefore removed from the data. A phase adjustment (see next section) is then made to correct for any instrumental phase shifts and the final result displayed on the monitor or stored in a data file.

VI. CALIBRATION

Calibration of the susceptometer is done in two steps. The first is to determine and remove the inherent response of the instrument itself as it varies with amplitude of the applied field, frequency, and temperature. This can be accomplished by measurement of a sample with a known dependence on these factors. The second step is the absolute calibration of the instrument at some suitable value of amplitude, frequency, and temperature via normalization of the measured in-phase and out-of-phase susceptibilities X' and X'' with a sample of known magnetic moment.

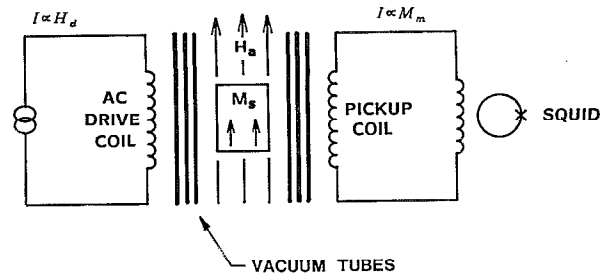


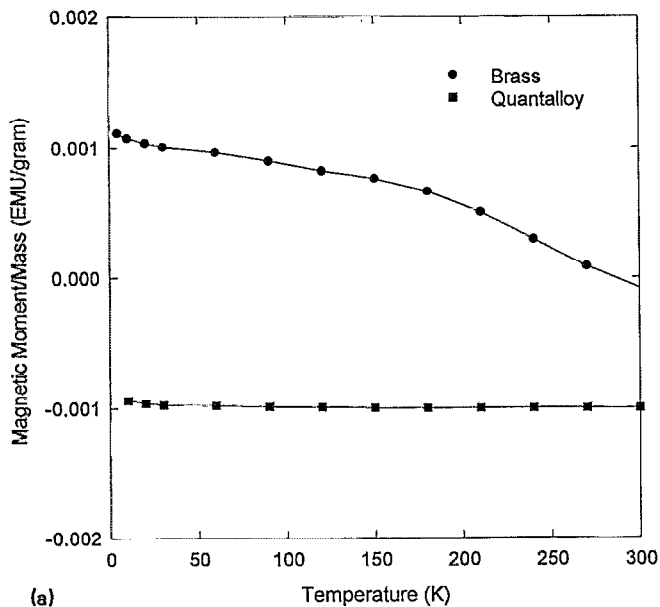
FIG. 4. Fields and moments referred to in Sec. V: H_d =desired applied field; H_a =actual applied field; M_s =induced sample moment; M_m =measured sample moment.

A. Intrinsic instrument response

Ideally, one would like a sample with a precisely calibrated amplitude and phase response as a function of both frequency and temperature for calibrating the intrinsic response of the instrument. In contrast to dc magnetic measurements, accurate calibration standards for ac measurements are not currently commercially available. However, by selecting a material whose imaginary component of the susceptibility X'' is zero, one can calibrate the amplitude and phase separately. Dysprosium (III) Oxide is an electrical insulator with a very large paramagnetic susceptibility. In the frequency range 0.001–1000 Hz its moment is in phase with the applied field; i.e., it is assumed that any component due to resistive or other dissipative mechanisms is too small to measure in our system. We can use this *a priori* knowledge that X'' is always zero for this sample to determine the phase response.

The intrinsic response of an instrument is determined by measuring two separate components: distortions in the field applied to the sample, and distortions in the measured sample moment. For clarity these are shown in Fig. 4. The desired magnetic field to be applied to the sample is H_d . The actual magnetic field in the sample space is the applied internal field H_a , which has an amplitude change and phase shift relative to H_d . The induced sample moment is M_s . The measured sample moment M_m has an amplitude and phase shift relative to M_s due to the intervening body of the instrument and measuring circuit. The determination and removal of the amplitude and phase shifts in H_a and M_m relative to H_d and M_s are discussed below. For samples with large susceptibilities, the effect of demagnetizing factors on the internal field of the sample must also be taken into account. The effect is negligible for samples with small susceptibilities, and will not be discussed further here. See Ref. 4 and references therein for a thorough discussion of demagnetizing factors, especially for superconductors and films.

Between the copper solenoid which produces the ac drive field and the sample are three concentric tubes made of a high resistivity material (quantalloy) which serve to thermally isolate the sample area from the liquid-helium bath. They produce small frequency and temperature-dependent attenuation and phase shift in the excitation field that is applied to the sample. In addition, the amplifier circuit which produces the ac drive current contains a 5 kHz one-pole filter. We made measurements of the dc magnetic moment of



these features may be directly determined by measuring the field in the sample space using a copper solenoid connected to a spectrum analyzer. It is found that the temperature dependence of H_a is sufficiently small over the range 2–400 K that no correction need be made to the applied field for changes in sample temperature. To account for the frequency dependence of the amplitude, the experimental data obtained from the test solenoid at 150 K are fit to a simple one-pole filter response with the rolloff frequency as the free parameter. The results are used to supply the necessary compensation to the amplitude of the applied field H_a .

It is not necessary to determine the absolute phase of the field applied to the sample since it has no physical significance. Changes in the phase of H_a due to frequency or temperature changes are taken care of during the removal of phase shifts in the measured signal M_m caused by the instrument itself, as described later in this section.

Distortions to the measured ac moment caused by the intrinsic frequency response of the instrument are the most difficult of the various effects to determine. Fortunately the frequency response is independent of amplitude of the ac drive field (note that this does *not* imply that the measured amplitude is independent of frequency!). Thus we need only consider calibration of the frequency and temperature dependence of the amplitude and phase of the measured signal.

Regarding temperature dependence, only the temperature of the inner vacuum sleeve and the sample chamber tube vary when the sample temperature is changed; the detection coils, various filters, and amplifiers present elsewhere in the circuit remain unchanged. At very low frequencies there is no change in the amplitude and phase shifts in the measured signal due to these tubes as a function of temperature. Thus we attribute any temperature-dependent effects measured at low frequencies to the sample and not the system. For example our calibration material dysprosium (III) oxide is paramagnetic and shows the usual $1/T$ dependence of its moment at low frequencies. Thus we normalize all frequency-dependent variations in the measurements to the low-frequency values at all temperatures.

Before the signal is digitized it passes through five filters with selectable ranges. Discontinuities in the frequency dependence of the measured signal from these filters are removed by a second-order interpolation procedure using a table generated during calibration. This is performed automatically by the instrument software.

The *a priori* knowledge that the phase of the susceptibility of dysprosium (III) oxide is zero ($X''=0$) is sufficient to calibrate the phase of the sample field as well as the phase shift between M_s and M_m because the phase shift in the applied field and the intrinsic phase shift of the instrument always appear together and do not need to be separately determined. Thus by setting the measured phase shift in M_m to zero for dysprosium (III) oxide we remove both individual phase adjustments from the data.

In addition to varying the ac field amplitude, temperature, and frequency, it is possible to apply dc magnetic fields up to 5 T in either direction along the sample chamber axis. The presence of a dc field produces small amplitude and phase shifts in the measured signal via field induced changes

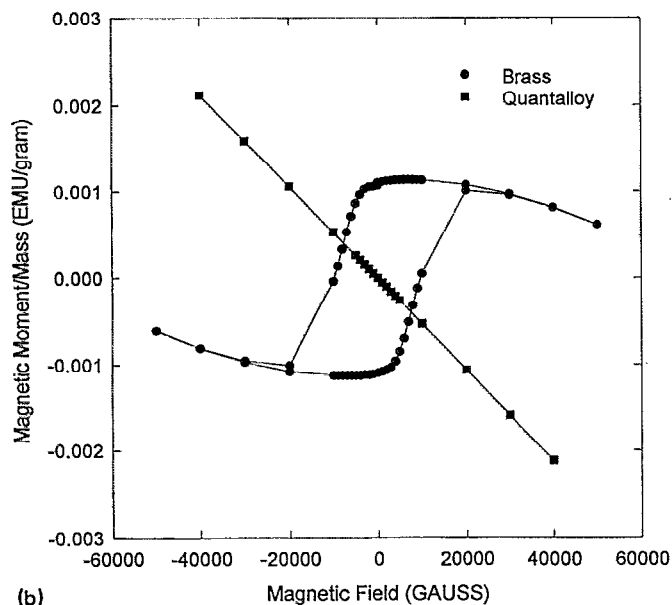


FIG. 5. Magnetic moment/mass of brass and quantalloy as a function of (a) temperature, measured at 1 T and (b) applied dc field, measured at a temperature of 10 K.

small samples of the quantalloy and of brass as a function of temperature and applied dc field in the sample chamber of the MPMS. In Fig. 5(a), we show the dependence of the magnetic moment of quantalloy compared to brass as a function of temperature at an applied field of 1 T. We see that the moment of the quantalloy is essentially independent of temperature compared to brass. The moment of the same samples for measurements over the range of -5 to 5 T at a temperature of 10 K is shown in Fig. 5(b). The nonhysteretic dependence on applied field of the alloy's moment is essential if an unambiguous correction is to be made in the applied field.

The frequency and temperature dependence of the amplitude of the magnetic field applied to the sample due to

in the screening properties of the superconducting magnet wire and the normal conductors present. These are corrected for by making absolute measurements of the signal at different values of the applied dc field with a test coil inserted into the sample area. At 5 T the measured ac field value is larger than that measured with no applied dc field by an amount varying from 0.3% at 10 Hz to 2% at 1 kHz, with a maximum phase shift of 4%. This effect is accounted for in the software controlling the ac drive coil so that the field applied to the sample is always the field specified by the user.

B. Absolute calibration

The absolute calibration of the system requires a sample known to have negligible frequency dependence in its measured moment, has a large susceptibility which is linear in the required range of fields, and has no screening currents which can change its effective shape. Again dysprosium (III) oxide is a suitable sample. The ac measurement system uses the same pickup coils and SQUID detection system as the dc system, which is calibrated from palladium reference standards supplied by the National Institute of Standards and Technology (NIST). Thus we calibrate the ac measurement by comparing it to a dc measurement. First the sample is measured at several low dc fields using the superconducting dc magnet. The measurement is then repeated at the same temperature using a dc field set by the ac solenoid. The measured susceptibility is normalized to the dc value in software, so that the measured value M_m agrees with the known sample moment M_s . The measurement is repeated in an ac field at very low frequency to verify that the ac value (which is entirely in phase with the applied field) agrees with that determined from the dc measurement.

Since sine wave generation and analysis are entirely digital, calibration of the absolute value of a measured phase is trivial since the wave period and the interval between data points are precisely known. The ultimate accuracy with which the phase may be determined is related to the stability of the crystal oscillator controlling all timing signals in the digital circuitry, and poses no limitations on the system.

If the inherent sensor noise of the SQUID is the limiting noise source, the system noise level can be estimated from the noise characteristics of the SQUID detector and the coupling factors between the SQUID and detection coils. In our apparatus the SQUID noise referenced to its input is about $6 \text{ pA}/\sqrt{\text{Hz}}$ (above 0.1 Hz), giving a detector sensitivity for a single SQUID reading of about $6 \times 10^{-12} \text{ A m}^2/\sqrt{\text{Hz}}$ referenced to the corresponding value of magnetic moment. That the system sensitivity reflects the noise characteristics of the SQUID detector is shown in the next section where data from measurements on several different systems are analyzed.

VII. EXPERIMENTAL RESULTS

Measurements have been performed with several different samples both during the calibration procedure and with the calibrated instrument in order to determine the system's range and capabilities for a variety of measurement conditions and types of samples. In Fig. 6 we show the results of repeated measurements of a dysprosium (III) oxide sample at

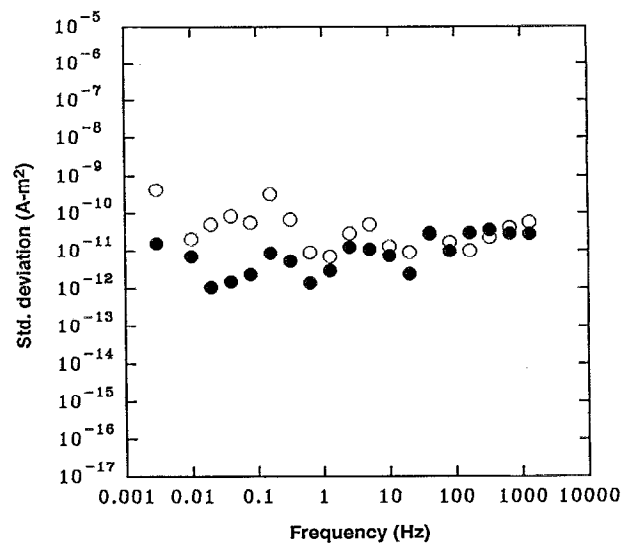


FIG. 6. Standard deviations for the average of four measurements of the moment of dysprosium (III) oxide as a function of frequency using an ac drive field of $5 \times 10^{-6} \text{ T}$. The closed circles are in the absence of an applied dc field and the open circles for an applied field of 1 T.

a temperature of 295 K and in dc magnetic fields of 0.0 and 1.0 T. The measurements were made with an applied ac field of $5 \times 10^{-6} \text{ T}$, at frequencies from 0.003 to 1300 Hz. The in-phase component of the moment is about $3 \times 10^{-9} \text{ A m}^2$. The data points are the standard deviations (SD) of four measurements of the in-phase component at each frequency above 0.01 Hz, and two measurements for the lower frequencies. The sinusoidal-looking variations for a given applied dc field result from variations in the number of digitized points per cycle used for the ac driving field, and the number of blocks of data averaged for each measurement. The empirical observation is that a larger number of points per cycle (as determined by the clock frequency and memory limitations) will result in a better resolution in determining the phase of the signal if there is an out-of-phase component, while having little effect on the SD, i.e., the amplitude resolution. Improvements in the amplitude resolution come from the increase in the number of blocks that can be averaged as the frequency increases, for a given clock speed. Similar results for the SD of the out-of-phase component (whose amplitude should be zero) indicate that these measurements represent approximately the noise limit of the system. Note the increase in SD for the higher dc field, especially at lower frequencies where the mechanical stability of the system becomes relevant. Note also the increase in the SD due to $1/f$ noise in the SQUID below about 0.1 Hz.

In Fig. 7 we show measurements of the moment of a single strand of superconducting niobium-titanium wire using an ac field of 10^{-6} T at a frequency of 1 Hz. The peak in the out-of-phase component at the transition is easily seen despite its being only a few times greater than the noise level of the system and three orders of magnitude less than the in-phase component below the transition. The phase of the imaginary component away from the transition switches randomly by 180° (as evidenced by its changing sign), which indicates this quantity is below the system's noise level.

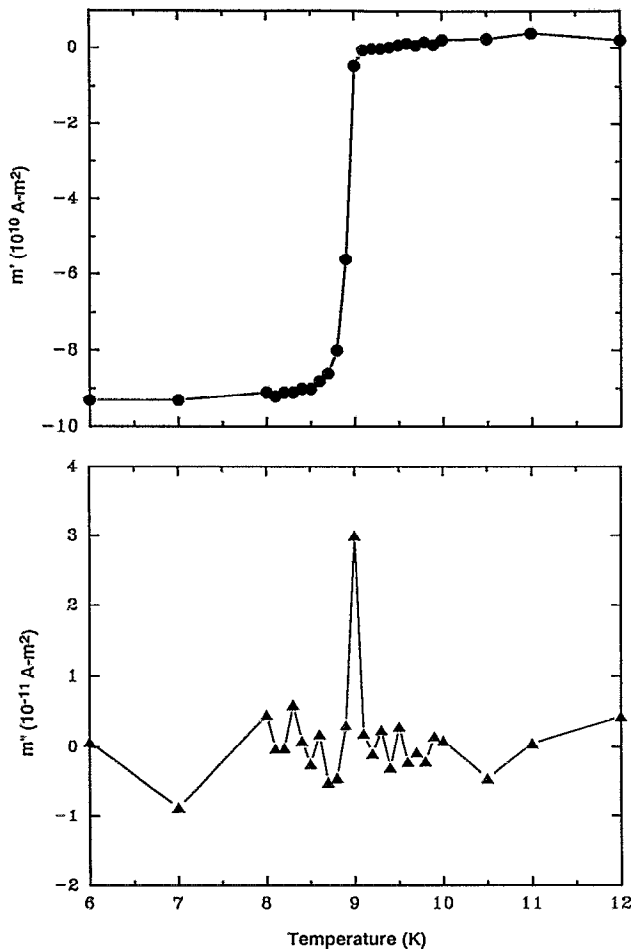


FIG. 7. In-phase and out-of-phase components of the moment of a single strand of NbTi wire 3 mm long and 80 μm diameter. The ac field was 10^{-4} T at a frequency of 1 Hz.

VIII. PERFORMANCE

Specifying the performance of the system is a complex subject because of the dependence on the conditions under which measurements are actually made. In order to discuss the performance of the instrument in a coherent fashion, we distinguish between relative and absolute measures of possible errors in measurement. We first consider under the heading of relative errors the quantities such as resolution and sensitivity of the detection system, and then discuss under the heading of absolute errors the reproducibility of measurements and accuracy of the system.

A. Relative errors

The sensitivity of the system can be defined as a gauge of its measurement threshold, i.e., the limit on how small a signal it can extract from the system noise. A related (and more general) quantity is the *resolution*, which is a measure of the system's ability to distinguish one moment from another, due either to the noise level or to the limitations of signal digitization. If the resolution of the system were limited by SQUID noise alone, it would be about 6×10^{-12} A m²/√Hz. One can in general use a smaller bandwidth by averaging many blocks of data during a signal measurement

or averaging the results of repeated measurements performed sequentially. One must be careful in assuming that a longer averaging time will always increase the resolution by reducing the standard deviation of several averaged measurements, however. For example, when operating at very low frequencies, if the averaging time is long compared to some characteristic time that the system can remain stable (between flux jumps of the SQUID, for instance, or due to thermal changes in the instrument), longer averaging times may actually increase errors in the measurement, or even make them impossible to carry out altogether. As seen in Fig. 6, where results on dysprosium (III) oxide are plotted, it is possible to improve the resolution of measurements with averaging, especially at frequencies below 0.1 Hz where the SQUID $1/f$ noise begins to increase.

B. Absolute errors

We define the repeatability of measurements with the system as the ability to get the same answer when making the same measurement at different times and under different conditions. The data shown in Fig. 6 for the SD of repeated measurements of dysprosium (III) oxide over a period of several days show the variations with applied dc field and frequency of the applied field used. Except for measurements where only two measurements (lowest frequencies) or fewer than four blocks of data were averaged, the maximum variation in repeated measurements over the whole frequency range and applied dc fields was about 2%, which is a measure of the absolute accuracy of the system.

The other measure of absolute accuracy is the system's ability to give the right answer for a known standard. Our calibration, as described above, is done against a known palladium standard for dc measurements, and therefore is accurate to the extent that this calibration standard is known.

ACKNOWLEDGMENTS

We wish to thank David Wright and Ralph Chamberlain of the Center for Solid State Science at Arizona State University and Larry Jones of the Materials Preparation Center at the Ames Laboratory for their assistance and advice in helping us fabricate components used in the susceptometer.

¹R. P. Giffard, R. A. Webb, and J. C. Wheatley, *J. Low Temp. Phys.* **6**, 533 (1972).

²J. Clarke, in *Superconductive Electronics*, NATO ASI Series Vol. **59**, edited by M. Nisenoff and H. Weinstock (Springer, Berlin, 1989), p. 87.

³Magnetic Property Measurement System, manufactured by Quantum Design, Inc., 11578 Sorrento Valley Road, San Diego, CA 92121.

⁴R. B. Goldfarb, M. Lelental, and C. A. Thompson, in Ref. 13, p. 49.

⁵A. F. Deutz, R. Hulstman, and F. J. Kranenburg, *Rev. Sci. Instrum.* **60**, 113 (1989).

⁶P. H. Müller, M. Schienle, and A. Kasten, *J. Magn. Magn. Mater.* **28**, 34 (1982).

⁷J. R. Owers-Bradley, Wen-Sheng Zhou, and W. P. Halperin, *Rev. Sci. Instrum.* **52**, 1106 (1981).

⁸D. H. Haines, Ph.D. thesis, Montana State University, March 1987.

⁹B. J. Dalrymple and D. E. Prober, *Rev. Sci. Instrum.* **55**, 958 (1984).

- ¹⁰R. E. Sager, A. D. Hibbs, and S. Kumar, *IEEE Trans. Magn.* **28**, 3072 (1992).
- ¹¹D. G. Xenikos and T. R. Lemberger, *Rev. Sci. Instrum.* **60**, 831 (1989).
- ¹²L. Koszegi, M. Foldeaki, and R. A. Dunlap, *Rev. Sci. Instrum.* **62**, 793 (1991).
- ¹³*Magnetic Susceptibility of Superconductors and Other Spin Systems*, ed-

ited by R. A. Hein, T. L. Francavilla, and D. H. Liebenberg (Plenum, New York, 1991), and references therein.

- ¹⁴P. Fabricatore, U. Gambardella, F. Gömör, R. Musenich, M. Occhetto, R. Parodi, and P. Pompa, *Rev. Sci. Instrum.* **62**, 1796 (1991).
- ¹⁵A. P. Ramirez, G. P. Espinosa, and A. S. Cooper, *Phys. Rev. Lett.* **64**, 2070 (1990).